CHEMICAL ENGINEERING TRANSACTIONS
VOL. 71, 2018
A publication of AIDIC
The Italian Association of Chemical Engineering
Online at www.aidic.it/cet
Guest Editors: Xiantang Zhang, Songrong Qian, Jianmin Xu

ISBN 978-88-95608-68-6; **ISSN** 2283-9216
DOI: 10.3303/CET1871064

Mathematical Model and Simulation of Chemical Thermosyphon based on Computational Fluid Dynamics

Xiaoming Han

Taishan Medical University, Taian 271016,China
anthoney@163.com

In this paper, based on computational fluid dynamics (CFD), the simulation study was conducted on the thermosyphon to construct the mathematical configuration of the thermosiphon. Then the CFD data simulation was performed for the thermosiphon and also the experimental comparison was made. The experimental results show that the thermosiphon has the best heat conduction effect under the condition of 500W energy supply and FR=0.4 filling rate. According to the simulation results, the increase of the FR has two different functions. First, the fluid volume becomes larger, and the boiling heat conduction effect can be deepened. Second, the liquid filling effect shall be enhanced and then the liquid surface be strengthened, which will cause many bubbles in the liquid phase of the evaporation zone and thus reduce the thermal conductivity; the most important is that with the liquid-filled effect increased, the gas phase area shall be increased and the pressure will be larger, so as to reduce the steam flow efficiency and overall system efficiency.

1. Introduction

Heat pipe is a high-efficiency heat exchange element that performs heat transfer by repeated phase change (evaporation, condensation) of a working fluid enclosed in a pipe. It can transmit a large amount of heat through its small cross-sectional area for long-distance transmission without external power. (Du et al., 2012). In the field of chemical industry, there are many needs for efficient and energy-saving heat exchange components (Cannistraro et al., 2018; Zhang et al., 2018). Due to their advantages in heat transfer, heat pipes have been widely used in many fields, such as furnace waste heat recoverer, steam generator, air preheater, and chemical reactors etc. (Chai et al., 2010; Al-Hindi et al., 1988; Gui et al., 2006).

As the most common type of heat pipe, the thermosyphon is no longer based on the liquid core, but on the effect of the original gravity; the transfer of matter and energy in this process is more diverse. The transfer of liquid back and forth inside the heat pipe, and the transfer of matter and energy are relatively diversified, and it is difficult to carry out only by the existing experiments, because of its more time-consumption and higher investments. Numerical simulation is not only efficient but also practical for heat pipe analysis. At present, many of the analyses are keen to use the method of accumulative accounting and experimental integration of data (Kaya et al., 2008; Bourdoukan et al., 2008).

At present, the scholars in many countries have begun to conduct a lot of explorations on heat pipes. They have obtained many effective research materials. But for the gas-phase and liquid-phase changes within heat pipes-the specific process of the transfer between relative matter and energy, it's difficult to achieve by the experiments and data collecting method. The model based on CFD for the gas and liquid phases changes within the heat pipe-relative matter and energy transfer, and its considerations are the necessary approaches to solve these problems, while using this approach can also greatly reduce the actual operation process and certain inputs. But now there has been no much full CFD analysis of the heat pipe, and also less analysis for the specific process of matter and energy transfer in the heat pipe. Therefore, the purpose of the paper is to provide a more complete coverage CFD model of the gas phase and liquid phase within the heat pipe-specific process of relative matter and energy transfer.

Please cite this article as: Han X., 2018, Mathematical model and simulation of chemical thermosyphon based on computational fluid dynamics, Chemical Engineering Transactions, 71, 379-384 DOI:10.3303/CET1871064

2. Theoretical basis

2.1 Introduction to FLUENT

FLUENT is the general-purpose software used to calculate fluid motion and energy transfer. It is also a widely used simulation system for calculating fluid mobility in the CFD approach. The paper is based on the Fluent of the FLUENT system in which the Gambit constructing the three-dimensional spatial structure and grid-structure is applied to draw the conclusion through the measurement calculation.

2.2 Theoretical basis for CFD calculation of evaporation and condensation

The gas phase inside the heat pipe is generally the engineering fluid and gas, and there are many energy and matter conversions in the interconnected areas between the flow states of the working fluids. Most of the energy conversions are most likely to be the changes in temperature, but there are also changes in latent heat resulting from changes in phases. According to the principle of energy and matter conversion, it can be seen that if there is a face-to-face relationship between the gas phase and the liquid phase, when the liquid phase molecules diffuse, liquid phase molecules will follow the region of the liquid film, and also may show the same gas phase boundary temperature as the liquid phase temperature near the droplet of liquid when they diffuse (Figure 1). The heat of saturated gas in the boundary layer has a crucial role in determining the vapor pressure and liquid vapor molecular content of the liquid phase in the boundary layer. Because the liquid-phase molecules are still diffused, many liquid vapours diffuse into the gas from the boundary layer, and many other liquid phases diffuse into the boundary layer (Peterson and Mallik, 1995; Mallik and Peterson, 1995).

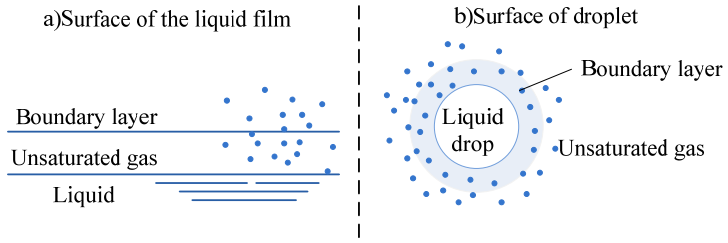

Figure 1: Gas-liquid heat and mass exchange

3. Thermosiphon experiment and numeral simulation

3.1 Experimental conditions and basic parameters

The gas-liquid phase closed thermosyphon analysis was applied in this paper. The specific process is shown in Figure 2:

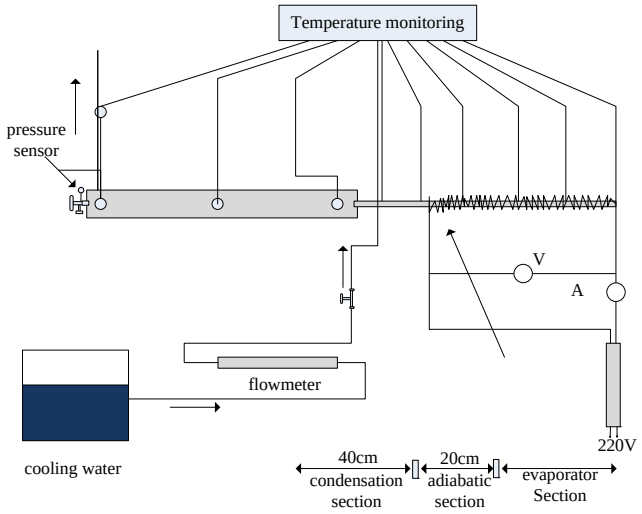

Figure 2: Test principle diagram of two-phase closed thermosiphon

The length of the thermosyphon was 1 meter, and the tube was φ=1.76 and Φ=2.0 cm. The condensation section above the thermosiphon was 0.4 meters long. The water flowing above was cold water. Its specific speed can be controlled by the control valve, and it is measured by the flowmeter with an error of ±0.19. Below the thermosiphon was an evaporation section of 0.4 meters: an electric heater initially making a certain thermal energy input was allowed to supply thermal energy to the evaporation section, and then the energy supplied to the evaporation section was set by the autotransformer. The adiabatic section was in the 0.2m central area of the thermosyphon. The thermocouple was arranged at the thermosiphon and then used to measure the temperature outside the condensing section, the adiabatic section, and the evaporating section at the measurement accuracy of 0.5±C°or so. Also, two thermocouples were used to determine the cooling inlet and outlet temperatures of the condensing section. The basic parameters of the thermosyphon are shown in Table 1.

Table 1: Basic parameters of hot siphon

The total length of heat pipe L_t/mm	950
Evaporation length L_e/mm	395
Adiabatic length L_a/mm	200
Length of condensation L_c/mm	390
Filling factor FR/%	20,40,70
Heat pipe diameter D_o/mm	20
Heat pipe diameter D_i/mm	17.4
Heat pipe wall thickness D_b/mm	0.74
Tubular product	Copper
Working medium	Water

3.2 Mathematical models and solving methods

The thermosiphon above has a very long and small geometric shape. In order to reduce the number of grids and enhance the calculation effect, the physical and mathematical configuration of the siphon heat pipe was constructed by using the axial symmetrical configuration formed in the plane system. With respect to the axisymmetrical geometrical configuration of the plane, the continuity equation is given as:

$$\frac{\partial}{\partial_t}(\alpha_v\rho_v)+\frac{\partial}{\partial x}(\alpha_v\rho_v v_x)+\frac{\partial}{\partial r}(\alpha_v\rho_v v_r)+\frac{\alpha_v\rho_v v_r}{r}=S_m \tag{1}$$

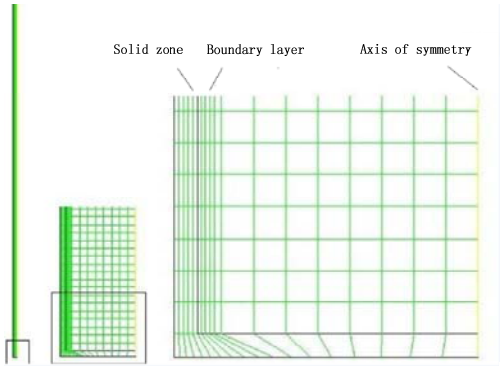

Figure 3: Grid division of the thermal siphon model

where, ρ_v is the gas phase density; α_v is the gas phase volume fraction, x is the axial coordinate, r is the radial coordinate, v_x is the axial velocity, v_r is the radial velocity, and S_m is the source term.

In the above experiment, the complete axisymmetric configuration for thermosiphon was constructed through two-dimensional cylindrical coordinates. The grid format is as shown in Figure 3. Through the cylindrical surface of 0.74 mm in size, an equal number of five-column grids were divided, and each grid had a width of 0.14mm. Since the wall surface was the main intermediate of heat conduction and the condensation section was in the outer wall area, the five-column grid was constructed by using the boundary layer in the liquid-variation part close to the wall surface. First, the first grid had a width of 0.1 mm, and then by increasing at the 1.20 contrast, the fifth grid was 0.20736mm wide. Therefore, the grid built on a certain solid portion and the

portion close to the zone boundary is very small, ensuring the accuracy of accounting and settlement. The other portion is determined by the grid planning size constructed by the Gambit system. The solid portion between the upper and lower configuration was the adiabatic section, which has little effect on the system construction and is distinguished by using a simple grid. The total number of configuration grids is 18,000.

3.2.1 Initial condition and boundary condition

For the interior of the thermosyphon, the boundary that cannot be moved was utilized, that is, the contents of the fluid and the wall does not allow relative sliding.

For the evaporation section, the power was used through the 500 watts of heat in the relative experiment. But, to apply FLUENT, the boundary environment must be changed to the heat flow density q_e at the unit of W/ m^2. The specific calculation is:

$$q_e = \frac{Q}{2\pi R_o L_e} \tag{2}$$

Substituting Q=500W, R_o =0.0095m, L_e =0.4m into formula (2), it's calculated to obtain the heat flux density q_e=20941.5W/ m^2.

The solid portion between the upper and lower configuration was the adiabatic section, which has little effect on the system construction, i.e. zero heat flow, so the heat flux density is believed to be zero.

For the condensation section, the temperature was reduced mainly by cooling water so as to cool down the vapour in the experiment. However, according to the actual development status, in the FLUENT system, the identified boundary environment of the condensation section is mainly for the convection heat transfer coefficient to fully simulate the heat transfer process. The corresponding convective heat transfer coefficient was determined in this way:

$$q_e = \frac{Q_c}{2\pi R_o L_e (T_c - T_w)} \tag{3}$$

where, Q_c represents the heat energy transferred from the condensation section; when the thermosyphon is heat-balanced, the heat energy transferred from the condensation section is close to the energy absorbed by the cooling. Besides, due to the remaining heat loss, the heat generated by the condensation section is lower than that in evaporation section. From Formula (2), it can be given as:

$$Q_c = Q_{out} = Q_{in} \cdot \eta_{max}\% \tag{4}$$

That is, Qc=500×70.6%=353W. Substituting R_o=0.0095m, L_e =0.4m, T_c=35°C, T_w=25°C into formula (3), the convective heat transfer coefficient of the condensation section q_e=1478W/(m^2·K) is obtained.

In the simulation stage, the fresh water was used for working medium, at the liquid rate FR=0.49. When the matter was constructed by FLUENT software, the surface tension between the solution ρ and the two phases along the interface was considered as the thermodynamic temperature T, which is mainly determined by the following formulas:

$$\rho_{liq} = -0.0022T^2 + 0.9237T + 919.8 \tag{5}$$

$$\sigma_{lv} = -2.3\times10^{-7}\times T^2 - 1.845\times10^{-5}T + 0.09805856 \tag{6}$$

3.2.2 Solving condition and methods

Under the two-phase flow conditions within similar thermosyphon, the instantaneous time was 0.0005s and the Krone number was set at 0.5.

To use the SIMPLE for pressure-velocity calculation, the semi-implicit approach is used specifically; first-order upwind scheme is adopted for momentum discreteness; Geo-Reconstruct interpolation and accounting is used to solve the volume fraction continuity equations, preventing from the unclear interfaces. If the residuals of m, E, and v are not greater than 0.0001, it can be believed that the actual accounting has started to be converged.

3.3 Calculation results and analysis

After accounting for 90 seconds, the thermosiphon completed the ground state and then started the study of its final data.

Table 2 lists the specific wall temperature value and CFD simulation wall temperature value under the condition of five hundred watts energy supply, the liquid filling rate FR=0.4. It's analysed that the average values of the calculated wall temperature and experimental wall temperature values are 6.5%, 6.3%, and 1.3% for the evaporation section, adiabatic section and condensation section respectively.

Table 2: The compare between experiment value and simulation value for wall temperature

Part	T_{EXP}(K)	T_{CFD}(K)	R_E (%)	$T_{EXP,AV}$ (K)	$T_{CFD,AV}$(K)	$R_{E,AV}$ (%)
evaporator	352.4	368.3	4.5	348.7	371.4	6.5
	346.4	370.7	7.0			
	347.6	374.1	7.6			
	348.2	372.5	7.0			
Adiabatic section	323.6	341.3	5.5	321.6	342.0	6.3
	319.5	342.6	7.2			
condensation section	305.2	310.6	1.8	307.6	311.8	1.3
	307.6	312.5	1.6			
	313.5	315.2	0.5			
	304.2	308.7	1.5			

For the outer wall surface temperature attached with thermosiphon, Fig.4 depicts the simulated results through CFD calculation and the experimental results. Red dots represent CFD simulated data, and black dots are the experimental values. There are four, two, and four different temperature values for the evaporation zone, adiabatic zone, and condensation zone respectively. It can be concluded from Figure 4 that all the experimental data and simulated temperature changes are consistent with each other. They're the differences between the simulated data under ideal conditions and the real data.

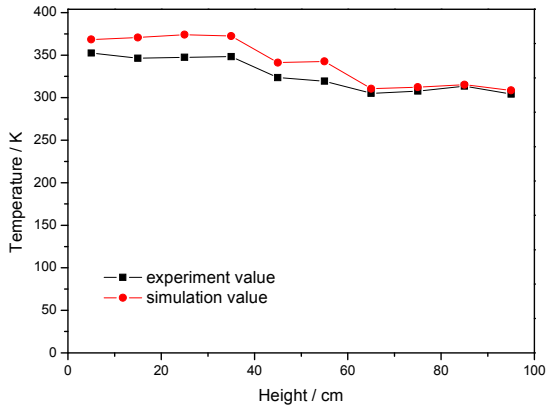

Figure 4: The compare between experiment value and simulation value for wall temperature

For the evaporation section, the data was simulated by continuously giving energy to the evaporation zone. In a specific case, it can avoid the temperature thermocouple and the electric heater to enter the evaporation zone. Therefore, in the liquid phase of the evaporation zone and the evaporation section, the heat exchange region of the inner wall of the heat pipe and the fluid section is not the same, and the heat exchange ability of the liquid section is stronger than the heat exchange region of the evaporation section. So, the temperature of the evaporation section is greater than that of the liquid region.

In the adiabatic zone, the simulated data and experimental data differ greatly. During the experiment, energy loss occurred in the adiabatic zone, so the wall temperature in the adiabatic zone decreased due to the increase in height at the beginning of experiment; however, in the simulation process, the heat loss was almost not taken into account. In other words, during the process, the adiabatic boundary allows the calculated temperature data to be roughly the same; the difference between these two simulated values is 0.49K. Experiments have shown that the wall temperature of the condensation zone becomes higher at a higher point, and that if the position of the thermosyphon siphon changes toward the upper part and the saturated steam goes to the highest position, then the hot gas is at the highest point of the condensing

section, causing the wall temperature of upper part to be higher, because it reaches the wall and returns. The gas-liquid phase diagram of the condensation section shows that the wall surface becomes thinner on the upper wall because of condensate fluid, and the film under the liquid film becomes thicker because of effect of gravity. With the thickness of the liquid film increased in the area where the uppermost sidewall surface is weak, the resistance of the liquid film decreases. Therefore, more heat can be transferred to the side wall surface, resulting in higher temperature at the uppermost wall surface of the condenser.

From above, it can be seen that it has two different functions to increase the filling rate FR. First, the volume of the fluid becomes larger, and the boiling heat conduction effect can be deepened; besides, a large area of working medium connecting the evaporation zone wall surface with the liquid shall emerge to improve the heat transfer efficiency, increase the evaporation effect, and then strengthen the effect of all heat pipes. Second, the liquid filling effect shall be enhanced and the liquid surface be strengthened, which will cause many bubbles in the liquid phase of the evaporation zone to reduce the thermal conductivity; and the most important is that with the liquid-filled effect increased, the gasr phase area shall be increased and the pressure will be larger, so as to reduce the steam flow efficiency and overall system efficiency. Therefore, based on the effect of the thermosiphon, the filling rate FR of the evaporating section must be appropriate. Under different heat conditions, the thermosyphon at the filling rate of FR=0.4 has the highest thermal property.

4. Conclusions

Based on computational fluid dynamics (CFD), the simulation study was conducted on the thermosyphon to construct the mathematical configuration of the thermosiphon. Then the CFD data simulation was performed for the thermosiphon and experimental comparison was made.

The experimental results show that the thermal siphon has the best heat conduction effect under the condition of 500W energy supply and FR=0.4 filling rate.

According to the simulation results, the increase of the FR has two different functions. First, the fluid volume becomes larger, and the boiling heat conduction effect can be deepened. Second, the liquid filling effect shall be enhanced and then the liquid surface be strengthened, which will cause many bubbles in the liquid phase of the evaporation area and thus reduce the thermal conductivity; the most important is that with the liquid-filled effect increased, the gas phase area shall be increased and the pressure will be larger, so as to reduce the steam flow efficiency and overall system efficiency.

References

Al-Hindi R.R., Khalifa A.M.A., Akyurt M., 1988, Simulation studies of the behaviour of a heat pipe-assisted solar absorption refrigerator, Applied Energy, 30(1), 61-80, DOI: 10.1016/0306-2619(88)90055-4

Bourdoukan P., Wurtz E., Joubert P., Spérandio M., 2008, Potential of solar heat pipe vacuum collectors in the desiccant cooling process: modelling and experimental results, Solar Energy, 82(12), 1209-1219, DOI: 10.1016/j.solener.2008.06.003.

Cannistraro M., Mainardi E., Bottarelli M., 2018, Testing a dual-source heat pump, Mathematical Modelling of Engineering Problems, 5(3), 205-210, DOI: 10.18280/mmep.050311

Chai B.Y., Min S., Li X.Y., Zhou SJ., Shi Y.C., 2010, Numerical simulation of oscillating heat pipe heat exchanger, International Journal of Food Engineering, 6(1), 61-64, DOI: 10.2202/1556-3758.1830.

Du J., Bansal P., Huang B., 2012, Simulation model of a greenhouse with a heat-pipe heating system, Applied Energy, 93(5), 268-276, DOI: 10.1016/j.apenergy.2011.12.069.

Gui X.H., Yuan X.G., Song X.G., Xu W.Q., 2006, Numerical modelling and simulation of heat pipe receiver, Aircraft Engineering and Aerospace Technology, 78(4), 315-320, DOI: 10.1108/17488840610675591.

Kaya T., Pérez R., Gregori C., Torres A., 2008, Numerical simulation of transient operation of loop heat pipes, Applied Thermal Engineering, 28(8), 967-974, DOI: 10.1016/j.applthermaleng.2007.06.037.

Mallik A.K., Peterson G.P., 1995, Steady-state investigation of vapor deposited micro heat pipe arrays, Journal of Electronic Packaging, 117(1), 75-81, DOI: 10.1115/1.2792070.

Peterson G.P., Mallik A.K., 1995, Transient response characteristics of vapor deposited micro heat pipe arrays, Journal of Electronic Packaging, 117(1), 82-87, DOI: 10.1115/1.2792072.

Zhang C.J., Guo Q., Sun J.L., Liu C., 2018, Comparative Analysis for Heat Transfer Performance of Heat Exchanger Single Tube Model with and Without Plug-in, Chemical Engineering Transactions, 66, 301-306, DOI: 10.3303/CET1866051